Current Biology, Volume *27*

Supplemental Information

Tissue-Specific Emission of (*E*)-α-Bergamotene Helps Resolve the Dilemma When Pollinators Are Also Herbivores

Wenwu Zhou, Anke Kügler, Erica McGale, Alexander Haverkamp, Markus Knaden, Han Guo, Franziska Beran, Felipe Yon, Ran Li, Nathalie Lackus, Tobias G. Köllner, Julia Bing, Meredith C. Schuman, Bill S. Hansson, Danny Kessler, Ian T. Baldwin, and Shuqing Xu

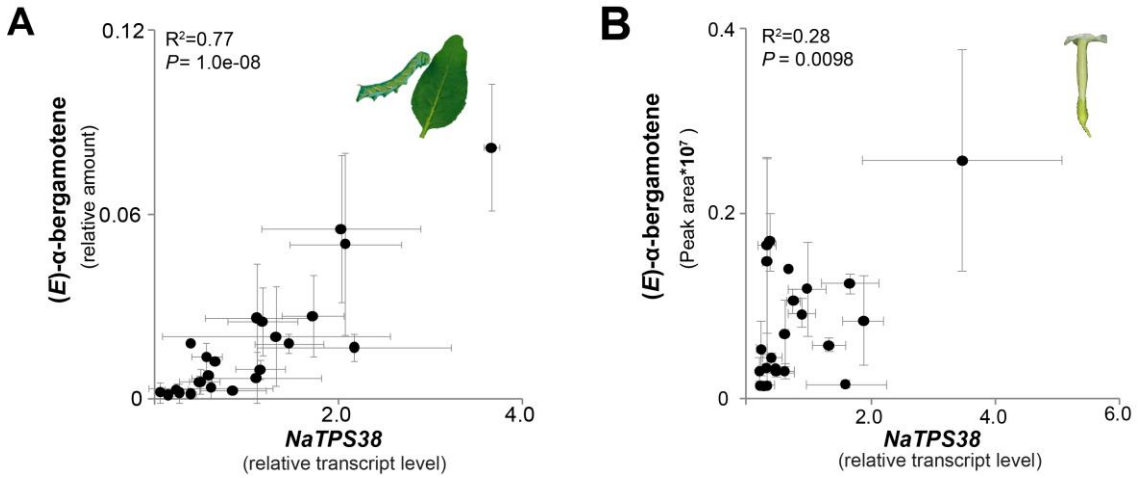

Figure S1. Among 23 natural accessions, relative transcript abundances of *NaTPS38* correlates with levels of (*E*)-α-bergamotene emission in both flowers (B) and herbivory-induced leaves (A), related to Figure 3.

The x-axis indicates the relative transcript abundance of *NaTPS38* measured at 4pm (leaves) or 10 pm (flowers); Y-axis refers to the relative amount of (*E*)-α-bergamotene measured between 12 and 4 pm (leaves) or between 9 and 10 pm (flowers). Data is shown as mean ±SD.

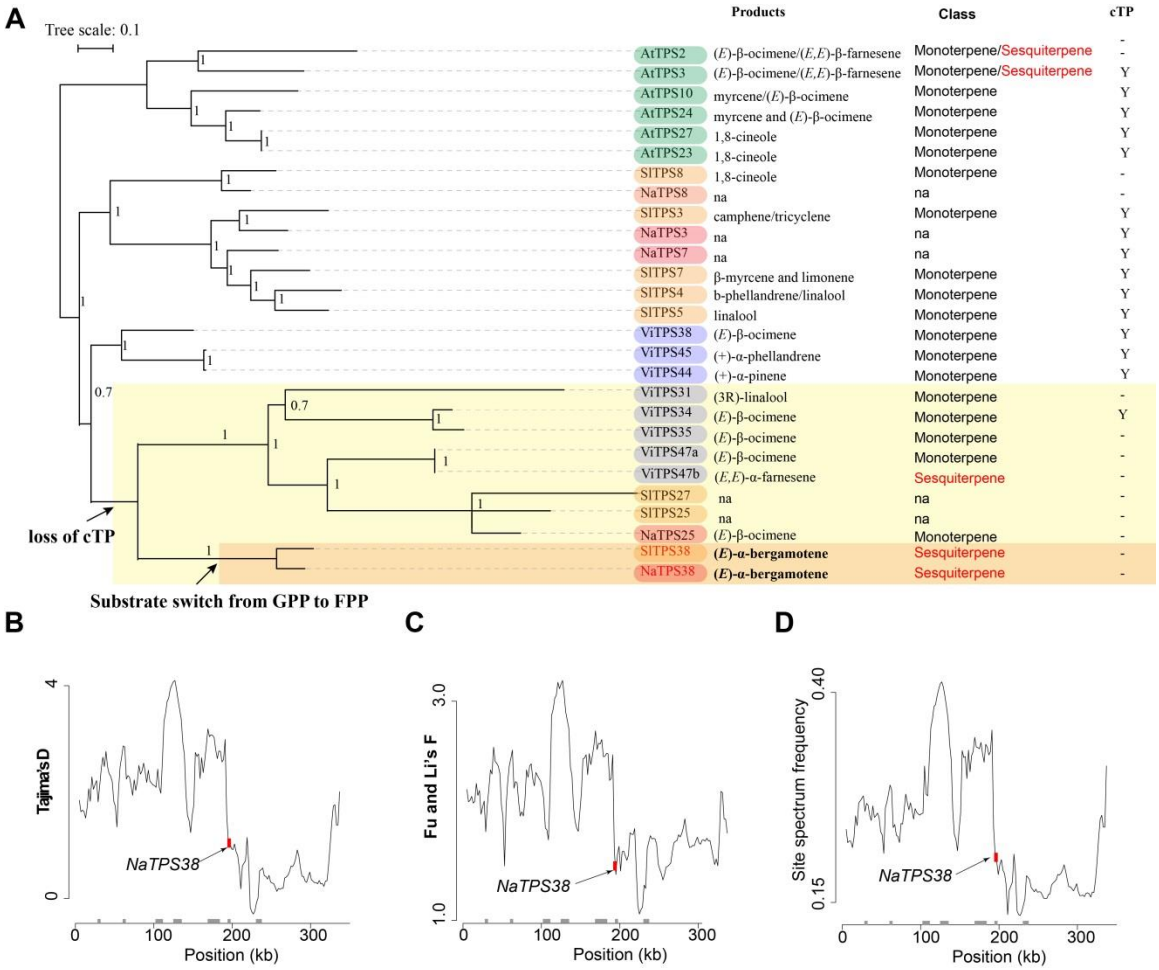

Figure S2. *NaTPS38* evolved from a monoterpene synthase and was under positive selection in *N. attenuata*, related to Figure 3.

A, a phylogenetic tree of genes from TPSb-clade in four plant species is shown. The number at each branch indicates an approximated *Bayesian* value. The predicted loss of chloroplast transit peptides (cTP) and substrate switching are shown on the tree. The leaf color of the phylogenetic tree refers to different species. Green: *Arabidopsis thaliana* (*At*); orange: *Solanum lycopersicum* (*Sl*); light blue: *Vitis vinifera* (*Vi*); pink: *Nicotiana attenuata* (*Na*). The products for each enzyme were summarized from previous publications and were classified as monoterpene or sesquiterpene. 'na' indicates that the product is unknown. The chloroplast transit peptides (cTP) for each TPS were predicted with Chloro P [S1]. 'Y' and '-' indicate predicted cTP presence and absence, respectively. **B-D**, a significant reduction of nucleotide diversity at the genomic region near *NaTPS38*. Sliding window plot of Tajima's D (**B**), Li and Fu's F (**C**) and site spectrum frequency (**D**) statistics are shown for the scaffold where *NaTPS38* is located. In each panel, the red bar depicts *NaTPS38*, and gray rectangles at the bottom depict locations of other protein coding genes. The genome-wide Tajima's D, Fu and Li's F and SFS are positive, which suggest either a population reduction in the past or the unique fire chasing behavior of *N. attenuata* resulting a subset of genetic diversity were collected from a large seed bank.

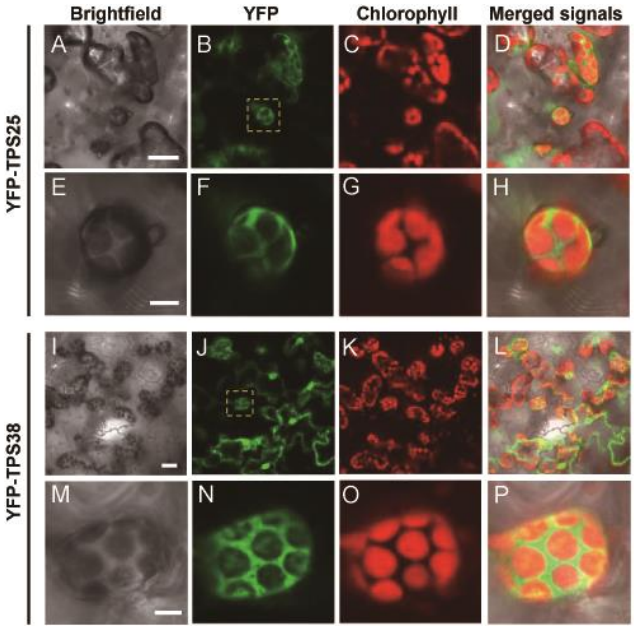

Figure S3. Subcellular localization of NaTPS25 and NaTPS38, related to Figure 3.
A-H, subcellular localization of YFP-TPS25; **I-P**, subcellular localization of YFP-TPS38. **E-H** and **M-P** are the zoomed view of **A-D** and **I-L**, respectively. The complete open reading frame of NaTPS25 (YFP-TPS25, A-H, T-V) and NaTPS38 (YFP-TPS38, **I-P**, **W-Y**) were fused downstream of YFP and transiently expressed in *N. attenuata* leaves. YFP fluorescence indicates the location of each fusion protein (green); the location of the chloroplasts was determined by chlorophyll autofluorescence (red). Merged signals provide a view of all fluorescent signals emitted from the leaf area. Scale bar in A, I: 20 μm; in E, M: 5 μm.

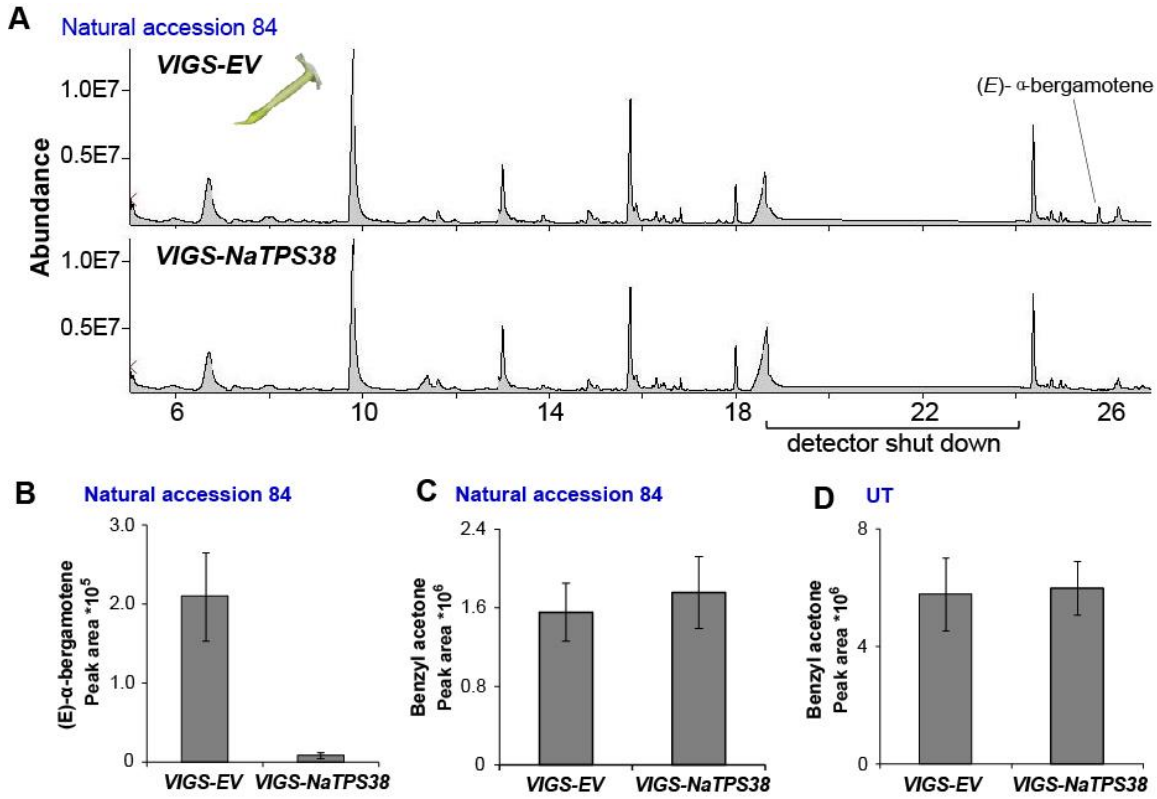

Figure S4. Silencing *NaTPS38* specifically reduced (*E*)-α-bergamotene emission in *N. attenuata* flowers, related to Figure 4.

A and **B**, silencing the expression of *NaTPS38* using VIGS specifically reduced emission of (*E*)-α-bergamotene, but not other volatiles in flowers. To prevent the overloading caused by the high amount of benzoyl acetone, the detector was shut down during the indicated retention time window. **C** and **D,** using a higher split ratio (1:10), we analyzed the benzyl acetone level from another PDMS tube used to sample the same flower (C-D). In comparison to VIGS-empty vector (EV) flowers, levels of benzyl acetone emission in flowers of VIGS-*NaTPS38* plants were not changed ($P > 0.1$, Student's-*t* test). To control the variation that might be caused by a different genomic background, the VIGS experiments were performed in two independent genotypes, UT and 84.

Table S1. Estimated effect size of identified QTL loci, related to Figure 2.
The QTL identifiers are indicated in Figure 2. SE refers to standard error.

		QTL1	QTL2
Linkage group		LG1	LG2
Position (cM)		90.69	296.95
Additive effect	SE	0.02	-0.16
	P value	0.95	0.02
	Estimate	1.16	**<0.001**
Dominant effect	SE	0.21	-0.20
	P value	**<0.001**	0.09

Table S2. TPS38 orthologue genes in different diploid solanaceous species, related to Figure 3.

Species	Gene ID	Data source
Petunia axillaris	Peaxi162Scf00931g00514	[S2]
Solanum melongena	Sme2.5_05438.1_g00002	[S3]
Capsicum annuum	CA02g17550	[S4]
N. tomentosiformis	NITOMv2_g07214	[S5]
N. obtusifolia	NIOBTv3_g07214	[S6]
N. sylvestris	NISLVv2_g07214	[S5]
N. attenuata	NIATv7_g07214	[S6]

Table S3. The response of *M. sexta* antenna and proboscis to (*E*)-α-bergamotene, related to Figure 4.
(*E*)-α-bergamotene elicited only a weak response on the antenna of *M. sexta* at relevant amounts, but was also detected by olfactory sensilla on the moth proboscis. The response of *M. sexta* antenna to (*E*)-α-bergamotene was measured using electroantennograms (EAG), the response of the proboscis sensilla was measured using single-sensillum recordings (SSR).

Antenna EAG			
Compound	**Sample size**	**Mean EAD amplitude [µV]**	**S.E.M**
Benzylacetone (2.98 µg)	5	516	73.6
(*E*)-α-bergamotene (0.1 µg)	5	112	30.1
Solvent control	5	60	17.9
Proboscis SSR			
Compound	**Sample Size**	**Δ Spikes/s**	**S.E.M**
Benzylacetone (2.98 µg)	3	22.5	2.95
(*E*)-α-bergamotene (0.1 µg)	4	15.5	2.48
Solvent control	4	1.75	1.25

Table S4. The kinetics of floral (*E*)-α-bergamotene emission from the natural accession 84 and the AI-RIL line 24A, related to Figure 4.

The emission was measured at three time points: 8-9 pm, 10-11 pm, 2-3 pm. Data are shown as mean ± SD.

Genotype	(*E*)-α-bergamotene (peak area)		
	8 -9PM	10-11 PM	2-3 AM
84	400,549 ± 112,740	190,231 ± 32077	155,462 ± 130,339
24A	89,648 ± 22,217	123,204 ± 36908	133,152 ± 127,914

Supplemental Experimental Procedures

Plant material

Seeds of *Nicotiana attenuata* Torrey ex. Watson (Solanaceae) natural accessions were collected by Ian T. Baldwin and collaborators in the southwestern United States and inbred for one generation in the glasshouse. Two genotypes, UT and AZ used for developing the mapping populations, have been self-fertilized for 30 and 22 generations in the glasshouse, respectively. To develop the AI-RIL population, UT and AZ were first crossed to generate F1 plants, which were then self-fertilized to generate 150 F2 plants. From F2 to F6, in each generation, we intercrossed ~150 progeny using a random mating and equal contribution crossing design [S7]. For generation F7, two seeds from each of the crosses at F6 were germinated and used for the single-seed descendent inbreeding process. In total, five generations of inbreeding were conducted.

Plant growth conditions

All seeds were germinated following the protocol described by Krügel *et al*. [S8]. Plants were grown under in glasshouse conditions (26 ± 1°C; 16h : 8h, light: dark) [S8]. For the VIGS and subcellular localization experiments, plants were grown in climate chamber under a constant temperature of 26 °C and 16h:8h (light: dark) light regime, and 65% relative humidity [S9].

*Measuring kinetics of herbivory-induced leaf, and floral (*E*)-α-bergamotene emission*

We measured the emission kinetics of wounding and *Manduca sexta* oral secretion (OS)-induced (*E*)-α-bergamotene in leaves of the 30th generation inbred UT plants at the rosette stage (35 d after germination). OS was collected on ice from *M. sexta* larvae reared on *N. attenuata* plants as previously described [S10]. To simulate herbivore attack, one stem leaf of each plant was wounded with a pattern wheel and 20 μL of 1:5 diluted OS was added to the puncture wounds at 8 am. After the OS treatment, the leaf was immediately enclosed into a plastic cup (ethylene terephthalate, ~300 mL), and three polydimethylsiloxane (PDMS) tubes were incubated into the cup to absorb the plant volatiles emitted from the leaf as described by Kallenbach *et al*. [S11]. To obtain temporally resolved quantitative data for (*E*)-α-bergamotene, the PDMS tubes were collected and replaced by three new ones at 4 h (12 pm), 8 h (4 pm), 12 h (8 pm), 16 h (12 pm), 20 h (4 am), 24 h (8 am), 28 h (12 am), and 32 h (4 pm in the next afternoon) after simulated herbivore attack, and kept in -20 °C until analysis. For each collection, the uninduced leaves from intact plants were used to measure constitutive emission levels of (*E*)-α-bergamotene.

We measured the emission kinetics of floral (*E*)-α-bergamotene in flowers of both UT and AZ plants (50 d after germination). As flowers of *N. attenuata* remain open for three consecutive days and the flower age affects the quantity of floral volatiles, in the morning (8 am - 9 am) of the day for the volatile trapping, all flowers which opened the day before were removed. For each biological replicate, two flowers of the same plant were taken at 6 pm, 8 pm, 10 pm, 12 pm, 2 am, 6 am, 10 am and 2 pm and placed into a 15 mL glass vial (Sigma), where two PDMS tubes were placed ~2 cm away from the corolla limb before the vial was sealed. The PDMS tubes were collected at 1 h after incubation and kept in -20 °C until analysis.

To further determine whether (*E*)-α-bergamotene was emitted from the inside or the outside of the corolla tube, we measured the floral bouquet of the whole flower as well as the bouquet of the corolla tube from the outside. For the bouquet of the whole flower, one flower was completely placed into a sealed glass vial (15 mL) together with a PDMS tube. For measuring the bouquet from the outside of corolla tube, the flower was inserted into the glass vial through a hole in the cap and the joint between the corolla tube and the hole was further sealed using a parafilm membrane to reduce the penetration of volatiles. In this setup, the whole corolla tube was inside the glass vial while the corolla limb and the corolla tube mouth were outside of the glass vial. Two PDMS tubes were placed into the glass vial for volatile collection for 1 h (between 8 pm and 9 pm) and the collected PDMS tubes were kept in -20 °C until analysis. The results showed that the outside of corolla tube only produced 4.9% of total floral (*E*)-α-bergamotene (peak area of whole flower bouquet: 779,498±53,775, peak area of bouquet produced by outer corolla tube: 38,349±14,903).

*Measuring floral and herbivory-induced leaf (*E*)-α-bergamotene among 23 natural accessions*

The same treatment and sampling method as mentioned above was used to measure both floral and herbivore-induced (*E*)-α-bergamotene from plants from 23 natural accessions. To measure herbivore-induced (*E*)-α-bergamotene emission, all plants (50 d after germination) were treated with an OS elicitation at 8 am and volatiles were trapped between 12 pm and 4 pm using PDMS tubes. To measure floral (*E*)-α-bergamotene emission, one flower from each plant (60 d after germination) was collected at 9 pm and 10 pm and placed into a glass vial together with two PDMS tubes. At the end of sample collection, both herbivore-induced leaves (at 4pm) and flowers (at 10 pm) were immediately flash frozen in liquid nitrogen and then kept at -80 °C until gene expression analysis.

*Sampling (*E*)-α-bergamotene in AI-RILs*

The herbivore-induced (*E*)-α-bergamotene emission of AI-RIL plants (55 d after germination) was measured similarly as described above. The elicitation by OS was performed between 8-9 am, and two PDMS tubes were placed in the cup and incubated with the induced leaves for 24 h. The collected PDMS tubes were then kept in -20 °C until analysis. In total, (*E*)-α-bergamotene was measured in 256 samples.

Floral and herbivory-induced leaf volatile analysis by TD-GC-MS

PDMS pieces were placed in TDU autosampler tubes for TD-GC-QMS analysis on a TD-20 thermal desorption unit (Shimazu) connected to a quadruple GC-MS-QP2010Ultra (Shimazu). Specifications for desorption, columns used, and the spectra reading and identification, were as described by Kallenbach *et al.*[S11] and Schuman *et al.*[S12]. For all of the herbivory-induced volatiles, a 1:20 split was used, while no split was used for floral volatile analysis. To avoid overloading the detector due to the high abundance of benzyl acetone (BA) and nicotine, for the floral volatile analysis, we specifically shut down the detector at the retention times of the BA and nicotine peaks. The abundance of BA and nicotine were then analyzed using the second PDMS tube collected from the same sample using the same method but with 1:10 split.

QTL mapping

The genotype information of all AI-RIL plants and the linkage map were obtained from the dataset reported earlier (Xu et al. in revision). The R package QTLRel was used for QTL mapping following the tutorial [S13]. Briefly, the relationship among different individuals was first estimated based on pedigree information. The peak area of each compound was log-transformed. Samples with missing genotype or phenotype information were removed. In total, 207 samples were used for QTL mapping. Then the variance of the traits within the population was estimated via "estVC" and missing information of the genotypes was imputed using function "genoImpute". The estimated trait variance and imputed genotypes were then used for the genome-wide scan. The empirical threshold was estimated based on 500 permutations. The additive and dominant effects of the candidate QTLs were estimated by fitting a multiple QTL model using the function "gls".

Measuring expression of NaTPS38 from 23 natural accessions

The expression of both floral and herbivory-induced *NaTPS38* was measured in the same samples that were used for measuring (*E*)-α-bergamotene emission using qPCR. Total RNA was isolated using TRIzol reagent (Invitrogen) according to the manufacturer's protocol. RNA samples were then treated with DNase-I (Fermentas) to remove genomic DNA. In total, ~1 μg total RNA from each sample was reverse transcribed into cDNA using SuperScript II reverse transcriptase (Thermo Fisher Scientific). The relative transcript accumulation of *NaTPS38* was measured using qPCR on a Stratagene MX3005P PCR cycler (Stratagene). For all qPCRs, the elongation factor-1A gene, NaEF1a (accession number D63396), was used as the internal standard for normalization [S14]. Forward and reverse primers used for qPCR are AGGGACAGCTCCTTCTCAAA and GGAAAGAGGAATGGGTTCAA, respectively. The coding sequence of *NaTPS38* is submitted NCBI under accession number XM_019369632.

To determine whether *NaTPS38* is expressed, PCR amplification was performed with Phusion Green High-Fidelity DNA polymerase (Thermo) using 40 PCR cycles to enable the detection of rare transcripts. The forward and reverse primers used are CAATGGATCTTAGGAGGTCA and TCAGGAAAGAGGAATGGGTTCAA, respectively.

To investigate temporal dynamics in the transcript accumulation of *NaTPS38* in *N. attenuata* flowers, the transcript abundance was measured at three time points: 6pm, 10pm and 2pm of the following day using plants of UT genotype. While the *NaTPS38* transcript abundance increased from 6 pm (1.41 ±

0.20) to 10 pm (2.60 ± 0.74), which is consistent with the observed (*E*)-α-bergamotene emission pattern (Figure 1), the highest transcript abundance was found at 2 pm of the following day (6.84 ± 0.74), the time point when (*E*)-α-bergamotene emission was low. The inconsistency between *NaTPS38* expression and (*E*)-α-bergamotene emission at 2 pm of the following day could result from several non-exclusive reasons: 1) post-transcriptional regulation might be involved in regulating the abundance and function of NaTPS38 protein during the day; 2), at 2 pm*, N. attenuata* flowers are mostly closed. However, most of (*E*)-α-bergamotene emissions were found to be emitted from the inner side of the corolla tube. Therefore, even when the *NaTPS38* proteins are highly abundant and (*E*)-α-bergamotene is produce by the corolla tube, the compound was not emitted to outside and was not measured by our method; 3) substrate availability is known to fluctuate diurnally and might also contribute to the disconnection between the expression of *NaTPS38* and floral (*E*)-α-bergamotene emission in *N. attenuata* [S15]. Certainly, the mechanistic regulation of *NaTPS38* and (*E*)-α-bergamotene emission would require additional investigations, and are beyond the scope of our manuscript.

Cloning and heterologous expression of NaTPS38

The complete open reading frame of *NaTPS38* was cloned from cDNA using the primer pairs tps38fwd/ (ATGGATCTTAGGAGGTCAGGAA/TCAGGAAAGAGGAATGGGTTCAA). The resulting PCR fragments were cloned into the vector pET200/D-TOPO® (Invitrogen, Carlsbad, CA, USA) and *E. coli* strain BL21 Codon Plus (Invitrogen) was used for heterologous expression. Expression was induced by addition of isopropyl-1-thio-D-galactopyranoside to a final concentration of 1 mM. The cells were collected by centrifugation at 4000g for 6 min, and disrupted by a 4 × 30 sec treatment with a sonicator in chilled extraction buffer (50 mM MOPSO, pH 7.0, with 5 mM $MgCl_2$, 5 mM sodium ascorbate, 0.5 mM PMSF, 5 mM dithiothreitol and 10% v/v glycerol). Cell fragments were removed by centrifugation at 14,000 g, and the supernatant was desalted into assay buffer (10 mM MOPSO, pH 7.0, 1 mM dithiothreitol, 10% v/v glycerol) by passage through an Econopac 10DG column (BioRad, Hercules, CA, USA).

Enzyme assays were performed in a Teflon®-sealed, screw-capped 1 ml GC glass vial containing 50 µL of the bacterial extract and 50 µL assay buffer with either 10 µM (*E*,*E*)-FPP or 10 µM GPP, 10 mM $MgCl_2$, 0.2 mM $NaWO_4$ and 0.1 mM NaF. A solid phase microextraction (SPME) fiber consisting of 100 µm polydimethylsiloxane (SUPELCO, Belafonte, PA, USA) was placed into the headspace of the vial for a 60 min incubation at 30°C and then inserted into the injector of the gas chromatograph for analysis of the adsorbed reaction products. GC-MS analysis was conducted using an Agilent 6890 Series gas chromatograph coupled to an Agilent 5973 quadrupole mass selective detector (interface temp, 250°C; quadrupole temp, 150°C; source temp, 230°C; electron energy, 70 eV). The GC was operated with a DB-5MS column (Agilent, Santa Clara, USA, 30 m x 0.25 mm x 0.25 µm). The sample (SPME) was injected without split at an initial oven temperature of 50°C (monoterpenes) or 80°C (sesquiterpenes). The temperature was held for 2 min, then increased to 160°C (monoterpenes) or 200°C (sesquiterpenes) with a gradient of 7°C min^{-1}, and further increased to 300°C with a gradient of 100°C min^{-1} and a hold of 1 min.

In addition, we also cloned and analyzed the enzymatic function of NaTPS25 using the same method mentioned above. The truncated version of *NaTPS25_AZ* (missing the first 13 codons) was amplified using primer pairs tps25fwd/rev. The result showed that NaTPS25 specifically produce (*E*)-β-ocimene (data not shown).

Measuring (E)-α-bergamotene emission from VIGS plants

The VIGS and leaf (*E*)-α-bergamotene measurements were carried out on the inbred line UT for *NaTPS38*. The inoculation was performed at 25 days after germination, and volatile trapping was started at 20 days after the inoculation. Before the volatile trapping, three leaves were sampled before any treatment to test silencing efficiency using primers: GAAGTTCAAACCGAGCCTTG (forward) and GGATTCATGTTCTCTCTTTTGTGA (reverse). Three more leaves, at the -1, 0 and +1 positions (indicating fully expanded to expanding leaves), were treated with 75 µg MeJA dissolved in 20 µL lanolin paste. This paste was applied at the base of the leaves at 12 pm, and after 1 h, half of these leaves were sampled to test the silencing efficiency. The whole shoot was then enclosed for volatile collection. The volatile analysis was carried out as described by Schuman *et al.*[S16] with the following modifications: plants received clean air filtered through activated charcoal at a rate of 600 mL/min and volatiles were sampled by pulling air through poropak Q filters at a rate of 300 mL/min . Eluents were analyzed using a

liquid autosampler on a GC-MS-QP2010Ultra (Shimazu). The methods for the processing of these samples follow the description in Kallenbach *et al*. [S11]. This provided a quantitative comparison between samples, so the same eluents were also run on a Varian CP-3800 GC-FID for more quantitation. The methods for separation, processing, identification and quantification of volatiles for these samples follow those published by Schuman *et al.*[S12]. The qualitative and quantitative data sets collected were inspected graphically for normality and homogeneity and fit an appropriate statistical model in R (either lm or gls). Pairwise statistical comparisons of dependent variables were then extracted through lsmeans, from the R package *lsmeans*.

VIGS silencing efficiency and flower volatile measurements were also carried out in the inbred UT (30^{th} generation) plants and an additional natural accession plants (84). Floral volatile trapping began 30 days after inoculation. On the day of volatile trapping, old flowers (opened before the trapping day) were removed in the morning (8 am-9 am). For each biological replicate, one flower was taken from the plant at 10 pm and placed into a 15 mL glass vial (Sigma), where two PDMS tubes were ~2 cm away from the corolla limb before the vial was sealed. PDMS tubes were collected after 1 h (11 pm) and immediately kept in -20 °C until analysis as described above.

Subcellular localization

The construction of 35S: *YFP-NaTPS25* and 35S: *YFP-NaTPS38* reporter fusions were carried out as described by Earley *et al*. [S17]. The open reading frame encoding *NaTPS25* and *NaTPS38* were amplified and introduced into pEarleyGate 104 to generate YFP fusion constructs. Primers used for cloning are: CACCATGGATCTTAGGAGGTCAGG (*NaTPS38* forward), TCAGGAAAGAGGAATGGGTTCAA (*NaTPS38* reverse), CACCATGCAGACACAAAAAGTTCA (*NaTPS25* forward) and AACGTGAATAGGCCGAGATT (*NaTPS25* reverse). Recombined plasmids were then transformed into *A. tumefaciens* strain GV3101 for subsequent plant transformation. Leaves of 3-weeks old *N. attenuata* were infiltrated with *A. tumefaciens* cells containing these constructs. To enhance the protein expression level of the terpene synthases, a P19 suppressor of gene silencing of *Tomato Bushy Stunt virus* (TBSV-P19) was co-expressed. YFP fluorescence was visualized 48 h following the inoculation with a Zeiss LSM 510 Meta confocal microscope (Carl Zeiss, Jena, Germany). The images were analyzed using LSM 2.5 image analysis software (Carl Zeiss, Inc.).

Molecular evolution of TPS38

We constructed a phylogenetic tree of the TPS-b clade using an in-house developed pipeline [S6, 18]. In brief, we aligned all coding sequences using MUSCLE (v.3.8.31) [S19] based on translated protein sequences with TranslatorX (v.1.1) [S20]. For all aligned sequences, all non-informational sites (gaps in more than 20% of sequences) were removed using trimAL (v1.4) [S21]. Then, PhyML(v. 20140206) [S22] was used to construct the gene tree with the best nucleotide substitution model estimated based on jModeltest2 (v.2.1.5) [S23] with the following parameter: -f -i -g 4 -s 3 -AIC -a. Support for each branch was calculated using the approximate *Bayesian* method.

The signature of positive selection on the branch of *TPS38* was estimated based on the ratio of non-synonymous (d*N*) and synonymous (d*S*) nucleotide substitution rate (ω) using PAML 4.7 [S24] package and ETE [S25] toolkit with the likelihood ratio test (LRT). Specifically, the branch of *TPS38* was marked as the
foreground branch and the rest of branches were considered as the background branch. Then we performed the LRT test between the free-branch model (b_free), which assumes different selection pressure between foreground branch and background branch and the M0 model, which assumes the foreground and background branches are under the same selection pressure.

To investigate the signature of selection at the population level, we analyzed the nucleotide diversity among 23 genotypes of natural accessions (Xu et al. unpublished data) using a sliding window. In brief, for each accession, ~ 8 x whole genome resequencing data were obtained using Illumina HiSeq 2000. All of SNPs were called using the method described in Xu et al. (submitted). The neutrality test was based on the sliding window (window=1000bp, jump=100 bp) of Tajima's D, Fu and Li' F tests and minor allele site frequency spectrum (SFS) using the R package "PopGenome" (v2.1.6) [S26]. The genome-wide Tajima's D, Fu and Li's F and SFS are positive, suggesting either a population reduction in the past or that the unique fire chasing behavior of *N. attenuata* resulted in only a subset of genetic diversity were collected from a large seed bank.

Determination of the amount of (E)-α-bergamotene required for M. sexta *moths Y-maze choice assay.*

To determine the amount of (*E*)-α-bergamotene in the *M. sexta* moth choice assay, we measured and compared the (*E*)-α-bergamotene released from one flower from 9 pm to 10 pm (23 natural accessions) and a filter paper disc supplied with 10µL different concentrations of (*E*)-α-bergamotene in the 15 mL glass vial (Sigma). The concentrations of (*E*)-α-bergamotene (x) and peak area (y) detected from PDMS tubes correlated well (R^2=0.9974, y=1E+08*x-207546). This correlation allowed us to calculate the amount of (*E*)-α-bergamotene required to mimic the release from flowers among natural populations. The calculated (*E*)-α-bergamotene was then adjusted according to the volume of the container used for the Y-maze assay (50 mL), which resulted in 10µL 0.05 mM (*E*)-α-bergamotene, the concentration of which is similar to the levels of emission in the flowers of the natural assession 382 but lower than the emission from assession 84, 179 and 384.

Antenna and proboscis electrophysilogy

Electroantenograms were performed by isolating the antenna of a three day old, male moth, which had been sedated at 5 °C. The two last flagellae on the tip of the antenna were also cut to increase conductivtiy and both ends of the antenna were placed into glass capillaries containing insect saline solution. The electrical responses of the antenna were recorded via Ag-AgCl wires, which were placed into the saline solution and connected to a ten times high impedance DC amplifier (Syntech, The Netherlands). The signal was then received by a digital/analog converter (Syntech, The Netherlands) and saved on a PC at a recording rate of 2.4 kHz. Odor stimuli were prepared by pipetting 10 µL of the odorant onto a filter paper, which was placed into a glass pipet. The stimulus was then applied by running an air flow of 0.2 L/min through the pipet into a humidified air stream of 0.8 L/min that was constantly applied to the antenna.

Single sensillum recordings on proboscis of *M. sexta* have previously demonstrated an olfactory function of the mSt4 sensillum [S27]. Here we used the same technique, placing one tungsten electrode as a ground into the proboscis of an immobilized, three-day-old, male moth. A second tungsten electrode was then used to penetrate the mSt4 sensillum. Signal amplification, recording and stimulus delivery was performed as described for the electroanntenograms. In contrast to a previous study, in which we did not show a response of the mSt4 sensillum to a mixture containing (*E*)-α-bergamotene, purified (*E*)-α-bergamotene was used in the present study. The results showed that the mSt4 sensillum is likely involved in the detection of (*E*)-α-bergamotene.

Proboscis choice assays

To examine the proboscis choice of *M. sexta* with (*E*)-α-bergamotene, we use a custom-built Y-maze system [S27]. For each assay, 10 µL 0.05 mM (*E*)-α-bergamotene solution (dissolved in hexane) or pure solvent control (hexane) were pipetted onto a filter paper disc placed in a 50 mL glass bottle. Filtered clean air was pushed into the bottle and the air flow at each Y-maze arm attained 0.1 L/min. To prevent the moths' antenna from contacting (*E*)-α-bergamotene, the air was removed from the opening of the Y-maze at a rate of 0.2 L/min. The moths were allowed to forage freely for 4 min. A video camera (Logitech C615) was used to record the movement of the moth proboscis. The corolla limb from a freshly cut *N. attenuata* flower was attached to the opening end of the Y-maze to promote the vision orientation and improve the probing accuracy of the moth to the Y-maze system.

Using the corolla limb from the freshly cut *N. attenuata* flower did not affect the results we obtained for three reasons: 1) we installed an air-suction at the very front of the Y-maze, directly behind the attached corolla limb. In such a setup, none of the volatiles emitted from corolla limb enter into the Y-maze that was designed to test the proboscis responses; 2), in each test, the same corolla limb was used to measure the responses in the treatment as well as in the control. Given the large sample sizes of the analysis (N=19 for the single compound assay and N=21 for the whole floral bouquet of the VIGS-*NaTPS38* plants), it is unlikely that the observed pattern was influenced by the corolla limb by chance; 3) consistent patterns were observed for the experiments of the single compound assay and of the whole floral bouquet assay (repeated twice). These experiments were performed at different times using corolla limbs from different batches of *N. attenuata* plants. From these data, we conclude that using the corolla limb of *N. attenuata* did not influence the results we observed. Furthermore, because in nature, *M. sexta* moths are attracted by the BA emitted by the corolla limb of *N. attenuata* flowers (antenna response), our experimental setup closely reflects real pollination behavior of *M. sexta* moths.

To examine the proboscis choice of *M. sexta* under a whole floral volatile background, we compared whole floral bouquet of VIGS-*NaTPS38* plants and control plants (VIGS-EV) in the same Y-maze system.

The floral VOC from VIGS-*EV* and VIGS-*NaTPS38* flowers were examined prior the choice experiments, which showed that the silencing of *NaTPS38* specifically reduced the emission of (*E*)-α-bergamotene but not other floral VOCs (Figure S4A-B). The Y-maze setup and data analysis were same as the mentioned above. To approximately represent the natural concentration of (*E*)-α-bergamotene in the corolla tube, we used 10 undamaged fresh flowers for each assay, since the total volume of the glass bottle is much bigger than the volume of the corolla tube, without multiple flowers, the concentration of (*E*)-α-bergamotene would be diluted to much lower level than the one in the corolla tube of a single flower.

We performed *M. sexta* proboscis choice assay under whole floral volatile background twice using two different genotypes (UT and 84), which produce different levels of BA (high in UT, low in 84) and (*E*)-α-bergamotene (low in UT, high in 84). Although the magnitude of the effects on probing behavior of *M. sexta* differed between these two genotypes, likely due to different amount of (*E*)-α-bergamotene produced between these two genotypes, both experiments consistently showed that silencing *NaTPS38* reduced the probing time of *M. sexta*.

It is noteworthy that the concentrations of (*E*)-α-bergamotene used in the single compound proboscis choice assay and the whole floral bouquet choice assay are different. Due to the dilution effects explained above, the estimated (*E*)-α-bergamotene concentration that *M. sexta* moth accessed from the whole floral bouquet assay is only ~1/50 the concentration used for in the single compound assays. As higher concentration results in stronger effects (as seen from effect magnitude difference between UT and 84), the observed effect from our whole floral bouquet assay is a conservative estimate.

M. sexta *moth pollination assay*.

To test the influence of (*E*)-α-bergamotene on *M. sexta* pollination behavior under a semi-natural condition, we used the AI-RIL line 24A which emits very low levels of (*E*)-α-bergamotene in comparison to other AI-RIL plants. The floral (*E*)-α-bergamotene emission level of the accession 84, which produced the highest level of floral (*E*)-α-bergamotene among examined accessions, was set as the upper boundary. For all measurement, anthers of unopened new flowers were removed at 6 am (before anthesis) from the plants.

We then measured the emission difference between plants of the genotype 24A and 84 at three time points: 8-9 pm, 10-11 pm and 2-3 pm. The floral (*E*)-α-bergamotene level in accession 84 was 2.76-fold higher than that of 24A at 8-9 pm, then decreased to a similar level as 24A at 2 am (Table S4). Based on the observed differences, we tested the emission of (*E*)-α-bergamotene in flowers of 24A that were supplemented with different concentrations of (*E*)-α-bergamotene mixed with nectar. We found that adding 0.02 µL (*E*)-α-bergamotene of a 1 mM stock in hexane mixed with 2 µL nectar (with 0.04 µL DMSO) to the flowers of 24A significantly increased the emission of (*E*)-α-bergamotene from the control (2 µL nectar with 0.04 µL DMSO and 0.02 µL hexane) (Control: 95,188 ± 26,822, (*E*)-α-bergamotene supplementation: 224,474 ± 15,220) but these levels still remain lower than the emission levels found in flowers of accession 84 (426,489 ± 128,196). Therefore this concentration was used for the *M. sexta* moth pollination assay in a tent in Jena between August and September 2016.

Data availability

The raw data for QTL mapping, kinetic of (*E*)-α-bergamotene emission in leaves and flowers and *M. sexta* probing assays are deposited in the figshare repository (https://figshare.com/s/d0745f2a91ce77bbf5ac).

Supplemental References

S1. Emanuelsson, O., Nielsen, H., and Von Heijne, G. (1999). ChloroP, a neural network-based method for predicting chloroplast transit peptides and their cleavage sites. Protein Sci. *8*, 978-984.

S2. Bombarely, A., Moser, M., Amrad, A., Bao, M., Bapaume, L., Barry, C.S., Bliek, M., Boersma, M.R., Borghi, L., Bruggmann, R., et al. (2016). Insight into the evolution of the Solanaceae from the parental genomes of *Petunia hybrida*. Nat. Plants *2*.

S3. Hirakawa, H., Shirasawa, K., Miyatake, K., Nunome, T., Negoro, S., Ohyama, A., Yamaguchi, H., Sato, S., Isobe, S., Tabata, S., et al. (2014). Draft genome sequence of eggplant (*Solanum melongena L.*): the representative *Solanum* species indigenous to the old world. DNA Res. *21*, 649-660.

S4. Kim, S., Park, M., Yeom, S.I., Kim, Y.M., Lee, J.M., Lee, H.A., Seo, E., Choi, J., Cheong, K., Kim, K.T., et al. (2014). Genome sequence of the hot pepper provides insights into the evolution of pungency in *Capsicum* species. Nat. Genet. *46*, 270-278.

S5. Sierro, N., Battey, J.N.D., Ouadi, S., Bovet, L., Goepfert, S., Bakaher, N., Peitsch, M.C., and Ivanov, N.V. (2013). Reference genomes and transcriptomes of *Nicotiana sylvestris* and *Nicotiana tomentosiformis*. Genome Biol *14*.

S6. Brockmöller, T., Ling, Z., Li, D., Gaquerel, E., Baldwin, I.T., and Xu, S. (2017). *Nicotiana attenuata* Data Hub (*Na*DH): an integrative platform for exploring genomic, transcriptomic and metabolomic data in wild tobacco. BMC Genomics *18*, 79.

S7. Rockman, M.V., and Kruglyak, L. (2008). Breeding designs for recombinant inbred advanced intercross lines. Genetics *179*, 1069-1078.

S8. Krügel, T., Lim, M., Gase, K., Halitschke, R., and Baldwin, I.T. (2002). Agrobacterium-mediated transformation of *Nicotiana attenuata*, a model ecological expression system. Chemoecology *12*, 177-183.

S9. Galis, I., Schuman, M.C., Gase, K., Hettenhausen, C., Hartl, M., Dinh, S.T., Wu, J., Bonaventure, G., and Baldwin, I.T. (2013). The use of VIGS technology to study plant–herbivore interactions. In Virus-Induced Gene Silencing. (Springer), pp. 109-137.

S10. Halitschke, R., Schittko, U., Pohnert, G., Boland, W., and Baldwin, I.T. (2001). Molecular interactions between the specialist herbivore *Manduca sexta* (Lepidoptera, Sphingidae) and its natural host *Nicotiana attenuata*. III. Fatty acid-amino acid conjugates in herbivore oral secretions are necessary and sufficient for herbivore-specific plant responses. Plant Physiol. *125*, 711-717.

S11. Kallenbach, M., Oh, Y., Eilers, E.J., Veit, D., Baldwin, I.T., and Schuman, M.C. (2014). A robust, simple, high-throughput technique for time-resolved plant volatile analysis in field experiments. Plant J. *78*, 1060-1072.

S12. Schuman, M.C., Barthel, K., and Baldwin, I.T. (2012). Herbivory-induced volatiles function as defenses increasing fitness of the native plant *Nicotiana attenuata* in nature. eLife *1*.

S13. Cheng, R., Abney, M., Palmer, A.A., and Skol, A.D. (2011). QTLRel: an R package for genome-wide association studies in which relatedness is a concern. BMC Genet. *12*, 66.

S14. Oh, Y., Baldwin, I.T., and Galis, I. (2013). A jasmonate ZIM-domain protein NaJAZd regulates floral jasmonic acid levels and counteracts flower abscission in *Nicotiana attenuata* plants. PLoS One *8*.
S15. Pulido, P., Perello, C., and Rodriguez-Concepcion, M. (2012). New insights into plant isoprenoid metabolism. Molecular Plant *5*, 964-967.
S16. Schuman, M.C., Palmer-Young, E.C., Schmidt, A., Gershenzon, J., and Baldwin, I.T. (2014). Ectopic terpene synthase expression enhances sesquiterpene emission in *Nicotiana attenuata* without altering defense or development of transgenic plants or neighbors. Plant physiology *166*, 779-797.
S17. Earley, K.W., Haag, J.R., Pontes, O., Opper, K., Juehne, T., Song, K.M., and Pikaard, C.S. (2006). Gateway-compatible vectors for plant functional genomics and proteomics. Plant J *45*, 616-629.
S18. Zhou, W., Brockmöller, T., Ling, Z., Omdahl, A., Baldwin, I.T., and Xu, S. (2016). Evolution of herbivore-induced early defense signaling was shaped by genome-wide duplications in *Nicotiana*. eLife *5*.
S19. Edgar, R.C. (2004). MUSCLE: multiple sequence alignment with high accuracy and high throughput. Nucleic Acids Res *32*, 1792-1797.
S20. Abascal, F., Zardoya, R., and Telford, M.J. (2010). TranslatorX: multiple alignment of nucleotide sequences guided by amino acid translations. Nucleic Acids Res *38*, W7-W13.
S21. Capella-Gutierrez, S., Silla-Martinez, J.M., and Gabaldon, T. (2009). trimAl: a tool for automated alignment trimming in large-scale phylogenetic analyses. Bioinformatics *25*, 1972-1973.
S22. Guindon, S., Delsuc, F., Dufayard, J.F., and Gascuel, O. (2009). Estimating maximum likelihood phylogenies with PhyML. Bioinformatics for DNA Sequence Analysis *537*, 113-137.
S23. Darriba, D., Taboada, G.L., Doallo, R., and Posada, D. (2012). jModelTest 2: more models, new heuristics and parallel computing. Nat. Methods *9*, 772-772.
S24. Yang, Z. (2007). PAML 4: phylogenetic analysis by maximum likelihood. Mol. Biol. Evol. *24*, 1586-1591.
S25. Huerta-Cepas, J., Dopazo, J., and Gabaldon, T. (2010). ETE: a python environment for tree exploration. BMC Bioinformatics *11*, 24.
S26. Pfeifer, B., Wittelsburger, U., Ramos-Onsins, S.E., and Lercher, M.J. (2014). PopGenome: an efficient Swiss army knife for population genomic analyses in R. Molecular biology and evolution *31*, 1929-1936.
S27. Haverkamp, A., Yon, F., Keesey, I.W., Missbach, C., Koenig, C., Hansson, B.S., Baldwin, I.T., Knaden, M., and Kessler, D. (2016). Hawkmoths evaluate scenting flowers with the tip of their proboscis. eLife *5*.